Nucleophilicity and P-C bond formation reactions of a terminal phosphanido iridium complex

Serrano, Á.L.; Casado, M.A.; Ciriano, M.A.; de Bruin, B.; López, J.A.; Tejel, C.

DOI
10.1021/acs.inorgchem.5b02301

Publication date
2016

Document Version
Final published version

Published in
Inorganic Chemistry

Inorganic Chemistry

Article

pubs.acs.org/IC

Nucleophilicity and P−C Bond Formation Reactions of a Terminal Phosphanido Iridium Complex

Ángel L. Serrano,[†] Miguel A. Casado,[†] Miguel A. Ciriano,[†] Bas de Bruin,[‡] José A. López,[†] and Cristina Tejel*[,†]

[†]Departamento de Química Inorgánica, Instituto de Síntesis Química y Catálisis Homogénea (ISQCH), CSIC-Universidad de Zaragoza, Pedro Cerbuna 12, 50009-Zaragoza, Spain

[‡]Homogeneous and Supramolecular Catalysis, van't Hoff Institute for Molecular Sciences (HIMS), University of Amsterdam, Science Park 904, 1098 XH Amsterdam, The Netherlands

Supporting Information

ABSTRACT: The diiridium complex [{Ir(ABPN$_2$)(CO)}$_2$(μ-CO)] (**1**; [ABPN$_2$]$^-$ = [(allyl)B(Pz)$_2$(CH$_2$PPh$_2$)]$^-$) reacts with diphenylphosphane affording [Ir(ABPN$_2$)(CO)(H)(PPh$_2$)] (**2**), the product of the oxidative addition of the P−H bond to the metal. DFT studies revealed a large contribution of the terminal phosphanido lone pair to the HOMO of **2**, indicating nucleophilic character of this ligand, which is evidenced by reactions of **2** with typical electrophiles such as H$^+$, Me$^+$, and O$_2$. Products from the reaction of **2** with methyl chloroacetate were found to be either [Ir(ABPN$_2$)(CO)(H)(PPh$_2$CH$_2$CO$_2$Me)][PF$_6$] ([**6**]PF$_6$) or [Ir(ABPN$_2$)(CO)(Cl)(H)] (**7**) and the free phosphane (PPh$_2$CH$_2$CO$_2$Me), both involving P−C bond formation, depending on the reaction conditions. New complexes having iridacyclophosphapentenone and iridacyclophosphapentanone moieties result from reactions of **2** with dimethyl acetylenedicarboxylate and dimethyl maleate, respectively, as a consequence of a further incorporation of the carbonyl ligand. In this line, the terminal alkyne methyl propiolate gave a mixture of a similar iridacyclophosphapentanone complex and [Ir(ABPN$_2$){CH═C(CO$_2$Me)−CO}{PPh$_2$−CH═CH(CO$_2$Me)}] (**10**), which bears the functionalized phosphane PPh$_2$−CH═CH(CO$_2$Me) and an iridacyclobutenone fragment. Related model reactions aimed to confirm mechanistic proposals are also studied.

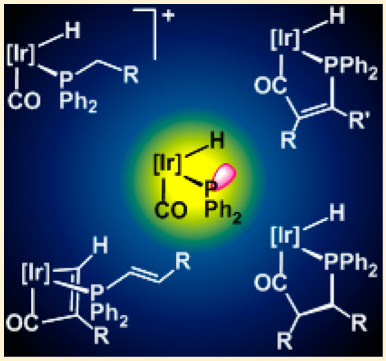

INTRODUCTION

Transition metal phosphanido complexes [M−PR$_2$] are valuable species proposed to be actively involved in modern catalytic transformations.[1] Among them, metal-mediated dehydrocoupling (DHC) of phosphane-boranes or primary and secondary phosphanes is providing an easy synthetic access to new inorganic materials, such as high molecular weight polyphosphaneboranes or phosphaneborane rings and chains.[2] Furthermore, [M−PR$_2$] species are highly relevant in both stoichiometric and catalytic P−E (E = B, C, Si, Ge) bond formation processes,[3] which usually afford P-containing products that are otherwise difficult to prepare by conventional methods.[4] As a matter of fact, phosphanido complexes of late transition metals have been recognized as active intermediates in catalytic hydrophosphanation (or hydrophosphorylation) of unsaturated substrates, especially with palladium-[5] and platinum-based catalysts.[6] Some studies involving rhodium-catalyzed DHC of phosphanes indicate that they occur through P−H bond activation processes, that is, by insertion of the metal into the P−H bonds of the substrates.[7] However, despite the relevance of this activation step, which should render terminal hydrido phosphanido species in the first stage, it is difficult to find isolated mononuclear hydrido organophosphanido metal complexes. Just a few complexes of rhodium,[7a] platinum,[8] nickel,[9] tantalum,[10] molybdenum, and tungsten,[11] coming from such a type of reaction, have been reported. The scarcity of terminal [M−PR$_2$] species is among other reasons due to their marked tendency to form phosphanido bridges. Indeed, the vast majority of these complexes (Co triad and after) are di- or polynuclear with bridging phosphanido moieties. Thus, a wide range of di[12]- and trinuclear[13] complexes of platinum and palladium have been reported; some of them promote interesting stoichiometric P−C,[14] P−N,[15] and P−O[16] bond formation reactions. Dinuclear rhodium and iridium phosphanido complexes have also been widely studied,[17] uncovering unusual coordination environments and bonding schemes, such as tetrahedral geometries for d^8-M configurations (M = Rh, Ir),[18] or square-planar in edge-sharing coplanar d^7-Rh compounds.[19]

On the contrary, terminal phosphanido compounds of iridium are very scarce. Isolated complexes include [Ir{N(SiMe$_2$CH$_2$PPh$_2$)$_2$}(CH$_3$)(PR$_2$)][20] (R = Ph, *m*-tolyl), [Ir(CO)(H)(L)$_2$X(PH$_2$)][21] (L = PEt$_3$, 1/2 dppe; X = Br, Cl), [IrCl$_2$(PMe$_2$Ph)$_3$(PH$_2$)],[22] and two recent examples with *fac*-L$_3$-iridium(I)[23] and *mer*-L$_3$-iridium(III)[24] scaffolds in which the phosphanido functionality is embedded within a tripodal ligand.

Received: October 6, 2015
Published: December 22, 2015

DOI: 10.1021/acs.inorgchem.5b02301
Inorg. Chem. 2016, 55, 828−839

Herein, we report the P−H bond activation of a secondary organophosphane by an iridium complex, which affords a terminal phosphanido hydrido compound involving direct oxidative addition of the R_2P−H bond to iridium. The new complex incorporates the original anionic hybrid scorpionate ligand $[(allyl)B(Pz)_2(CH_2PPh_2)]^-$ ($[ABPN_2]^-$, Pz = pyrazolate) that displays three different arms suitable for coordination.[25] Some reactions involving the new Ir−PPh_2 bond as well as the molecular and electronic structure of the complex are also reported.

RESULTS AND DISCUSSION

Addition of diphenylphosphane ($PHPh_2$) to the carbonyl-bridged dinuclear iridium(I) complex $[\{Ir(ABPN_2)(CO)\}_2(\mu\text{-}CO)]$[25a] (**1**) produces an immediate reaction to give the mononuclear hydrido phosphanido iridium(III) complex $[Ir(ABPN_2)(CO)(H)(PPh_2)]$ (**2**) (Scheme 1), isolated as a pale-yellow microcrystalline solid in 92% yield after workup.

Scheme 1. Synthesis of the Hydrido-phosphanido Iridium(III) Complex (2)

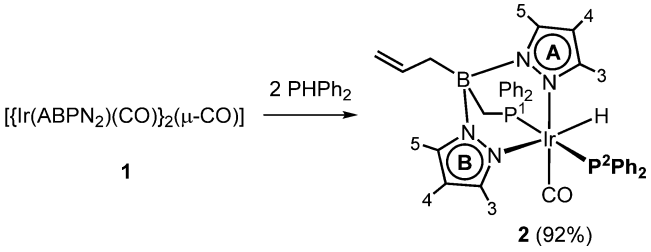

Complex **2** crystallized in a centrosymmetric space group ($P2(1)/n$), so that the crystal contains the racemic mixture. The enantiomer *OC*-6-25-*C* is shown in Figure 1. In the complex, the iridium atom lies at the center of a slightly distorted octahedron, bound to the scorpionate ligand in a $\kappa N,\kappa N',\kappa P$-mode, the hydride, the carbonyl, and the phosphanido ligands. Both phosphorus atoms are mutually *trans*, while the carbonyl and hydrido ligands are located *trans* to the nitrogen atoms of the pyrazolyl rings. The strong *trans* influence of the hydride ligand is reflected in a longer Ir−N3 bond distance when compared to the Ir−N1 distance, *trans* to the carbonyl ligand (Figure 1). Simultaneously, the phosphanido Ir−P2 bond distance is also clearly longer than the corresponding Ir−P1 bond distance of the phosphane arm of the tripodal ligand. This short/long bonding scheme for *trans*-R_3P−M−PR_2 moieties in square-planar/octahedral complexes is quite common,[26] and has been attributed to the stronger *trans* influence of the phosphane ligand.[22] Electronic repulsion between the phosphanido lone pair and the filled iridium d_{xy}, d_{yz}, and d_{xz} orbitals might also play a role.

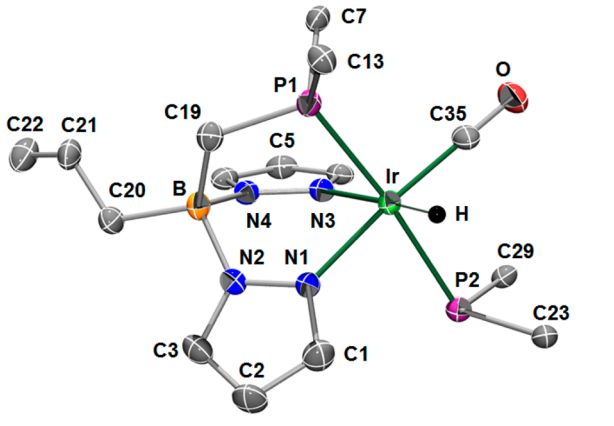

Figure 1. Molecular structure (ORTEP at the 50% level) of complex **2**. H atoms and the solvent of crystallization have been removed, and only the C^{ipso} atoms of the phenyl groups are shown for clarity. Selected bond distances (Å) and angles (deg): Ir−P1, 2.348(1); Ir−P2, 2.436(1); Ir−N1, 2.094(3); Ir−N3, 2.161(3); Ir−C35, 1.838(5); Ir−H, 1.54(4); C23−O, 1.139(5); P1−Ir−P2, 174.21(4); N1−Ir−C35, 175.0(2); N3−Ir−H, 176.2(16); C23−P2−Ir−N1, 104.4(2); C29−P2−Ir−N3, −61.8(2).

Figure 2 shows two views of the molecule along the P2−Ir−P1 axis highlighting the eclipsed conformation of the P1−C7

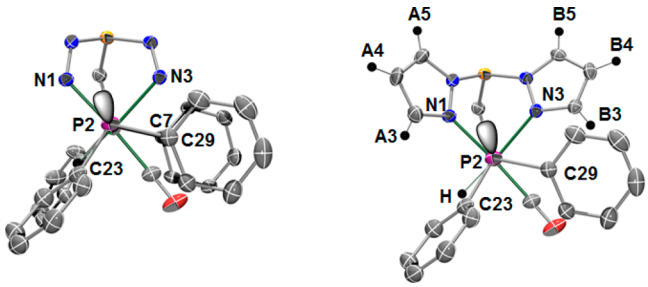

Figure 2. Two views of complex **2** along the P1−Ir−P2 axis.

with P2−C29 bonds and P1−C13 with P2−C23 bonds. The lone-pair on phosphorus is placed between both pyrazolate rings. Accordingly, quite different torsion angles C23−P2−Ir−N1 and C29−P2−Ir−N3 (Figure 1) were observed.

The stereochemistry of **2** in solution was assessed through a combination of NMR multinuclear experiments. Two well-separated doublets ($^2J_{P,P}$ = 97 Hz) observed in the $^{31}P\{^1H\}$ NMR spectrum reveal that both phosphorus atoms are located in mutual *trans* positions. However, the value of the coupling constant was found to be considerably smaller than that typically observed for *trans*-phosphane ligands (ca. 300−400 Hz), which can be attributed to a substantial reduction in the s-orbital character of the Ir−PR_2 bond as compared to Ir−PR_3.[22,26d,27] Moreover, the NMR data (see the Supporting Information) reflect a restricted rotational motion around the Ir−P2 bond and a structure close to that observed in the solid state. The relatively static nature of the molecule observed in solution contrasts with the typical dynamic behavior observed for M−PR_2 complexes, for which both phosphorus inversion and rotation around the M−PR_2 bond have been reported to be low-energy processes.[28]

The geometry of complex $[Ir(ABPN_2)(CO)(H)(PPh_2)]$ (**2**) was also optimized with DFT (b3-lyp, def2-TZVP, see the Supporting Information). Apart from somewhat longer Ir−L distances (which is common in DFT), the main difference between the optimized geometry and the X-ray structure is a slight reorientation of the phosphanido ligand, rotated somewhat around the Ir−P2 bond in the DFT optimized geometry.

The phosphanido lone pair has a large contribution to the HOMO of complex **2**, thus indicating nucleophilic character of this ligand. Interestingly, the LUMO of **2** is not located at the metal, but is centered at one of the phenyl groups of the neutral phosphane ligand (Figure 3). As can be expected, both the total atomic 3s-orbital population (1.48) and the total atomic 3p-orbital population (3.02) of the anionic phospanido ligand P

DOI: 10.1021/acs.inorgchem.5b02301
Inorg. Chem. 2016, 55, 828−839

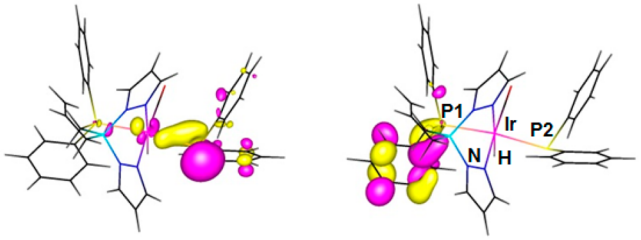

Figure 3. HOMO (left) and LUMO (right) of complex **2** (b3-lyp, def2-TZVP).

atom are larger than those of the neutral phosphane ligand P atom (3s 1.20; 3p 2.63). The DFT calculated Ir−P bond order (Wiberg) of the phosphanido donor (0.86) is stronger than that of the neutral phosphane donor (0.67), despite the longer (calculated and experimental) Ir−P2 bond as compared to the Ir−P1 bond. The Wiberg Bond Index (WBI) is a density-matrix-based quantum chemical descriptors of the bond order, and reflects both the strength and the covalency/polarity of a bond. WBI bond orders of 1 are typically only observed for nonpolarized σ-bonds, with substantially smaller values for polarized σ-bonds.[29] Because metal−ligand bonds are intrinsically polarized toward the ligand, metal−ligand WBI values between 0 and 1 are expected for M−L bonds with σ-donating ligands such as the phosphanido and phosphane donors under consideration. The increased WBI of the Ir−P bond for the phosphanido donor as compared to the phosphane donor reflects a stronger covalency and stronger Ir−P σ-bond.

The overall reaction leading to complex **2** involves the cleavage of the dinuclear complex **1** by coordination of the secondary phosphane and the oxidative-addition of the P−H bond to the iridium centers. Monitoring the reaction by NMR indicated no changes below −20 °C; above this temperature, a gradual transformation of **1** into **2** was readily observed, but no intermediates were detected. Nonetheless, the origin of the hydrido ligand in **2** was confirmed in a straightforward manner by monitoring the reaction of **1** with $PDPh_2$ by ^2H NMR, which gave $[Ir(ABPN_2)(CO)(D)(PPh_2)]$ (**2**-d_1). This information confirms the iridium-mediated scission of the P−H bond and rules out any other considerations about the origin of the hydrido ligand.

The product from the first step of the reaction of $[\{Ir(ABPN_2)(CO)\}_2(\mu\text{-}CO)]$ (**1**) with $PHPh_2$ would be the mononuclear complex $[Ir(ABPN_2)(CO)(PHPh_2)]$ (**A**), similar to the previously reported phosphane counterpart $[Ir(ABPN_2)(CO)(PPh_3)]$.[25a] The latter was found to exist as a mixture of two isomers in solution in equilibrium, involving the trigonal bipyramidal (*TBPY*) species, with one of the pyrazolyl groups and the carbonyl at the axial positions, and the square-planar (*SP*) with the two phosphorus atoms in a *trans* disposition. Such type of equilibrium has also been observed for related complexes with hybrid scorpionate ligands decorated with allyl groups.[30] Consequently, a similar equilibrium can be expected for complex $[Ir(ABPN_2)(CO)(PHPh_2)]$ (**A**, Scheme 2).

Both isomers, **A**-*TBPY* and **A**-*SP*, were optimized with DFT (b3-lyp, def2-TZVP), and their structures are shown in Figure 4. For **A**, the energy difference between the *SP* and *TBPY* isomers turned out to be quite big. The **A**-*SP* geometrical isomer is 14.3 kcal mol^{-1} more stable than **A**-*TBPY*, and accordingly (in contrast to $[Ir(ABPN_2)(CO)(PPh_3)]$) only **A**-*SP* should be present in appreciable amounts for $[Ir(ABPN_2)(CO)(PHPh_2)]$ species **A**. This is likely a reflection of the

Scheme 2. Equilibrium between Complexes A-*TBPY* and A-*SP*[a]

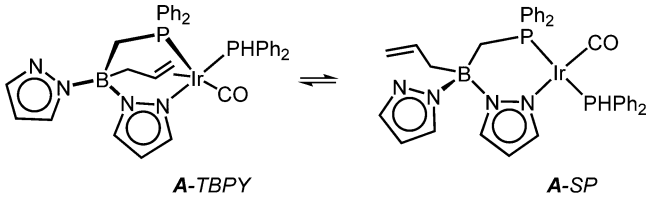

[a]A similar equilibrium was previously observed for $[Ir(ABPN_2)(CO)(PPh_3)]$-*TBPY* and $[Ir(ABPN_2)(CO)(PPh_3)]$-*SP*.

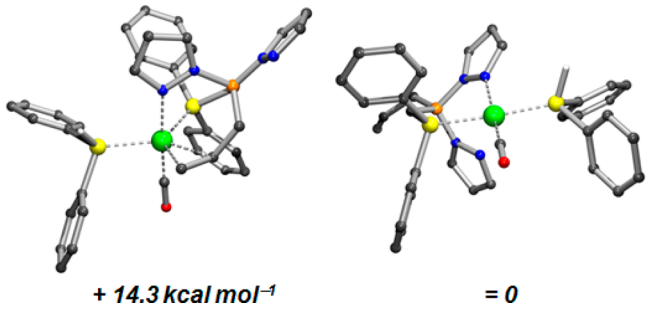

Figure 4. DFT-optimized (b3-lyp, def2-TZVP) structures of **A**-*TBPY* (left) and **A**-*SP* (right). Hydrogen atoms omitted, except for the PH hydrogen atom of the $PHPh_2$ ligand.

stronger donor capacity of the $PHPh_2$ ligand as compared to PPh_3.

The subsequent oxidative addition of the P−H bond from **A**-*SP* via **TS1** to form the hydride complex **2** was also computationally investigated (b3-lyp, def2-TZVP), revealing a moderate transition state barrier (**TS1**) of $\Delta G^{\ddagger}$ = +22.1 kcal mol^{-1} (relative to **A**-*SP*). The structure of **TS-1** (Figure 5)

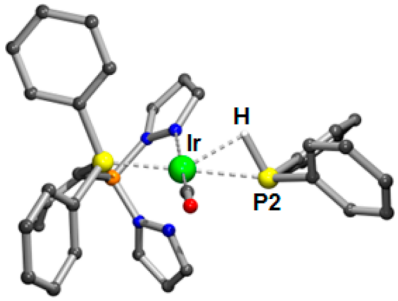

Figure 5. DFT-optimized (b3-lyp, def2-TZVP) structure of **TS1**. Hydrogen atoms omitted, except for that of the $PHPh_2$ ligand.

shows the hydrogen between phosphorus and iridium (P−H distance, 1.486 Å; Ir−H distance, 2.053 Å; corresponding distances in **A**-*SP*,: P−H distance, 1.413 Å; Ir−H distance, 3.182 Å). The free pyrazole donor approaches to iridium from 2.871 Å in **A**-*SP* to 2.623 Å in **TS-1**, showing partial oxidation from Ir^{I} to Ir^{III} in **TS-1**, and partial coordination of the pyrazole donor, which likely plays a role in stabilization of the transition state (anchimeric effect).

In principle, an intermediate with a σ-coordinated P−H bond could also be considered as being the precursor complex to **TS1** (instead of **A**-*SP*). However, all attempts to optimize complexes with a σ-coordinated P−H bond to iridium converged back to geometries with a P-coordinated phosphane Ph_2PH ligand without any interaction between the hydrogen

DOI: 10.1021/acs.inorgchem.5b02301
Inorg. Chem. 2016, 55, 828−839

Scheme 3. Reactions of $[Ir(ABPN_2)(CO)(H)(PPh_2)]$ (2) with HBF_4, MeOTf, and O_2

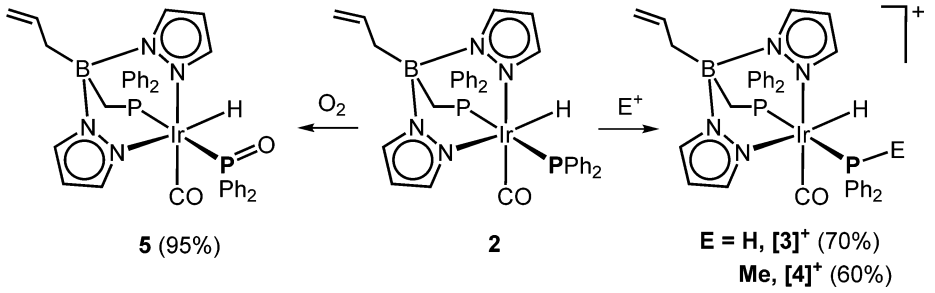

Scheme 4. Reaction of $[Ir(ABPN_2)(CO)(H)(PPh_2)]$ (2) with Methyl Chloracetate To Give Either Complex $[6]PF_6$ or Complex 7 and the Free Phosphane

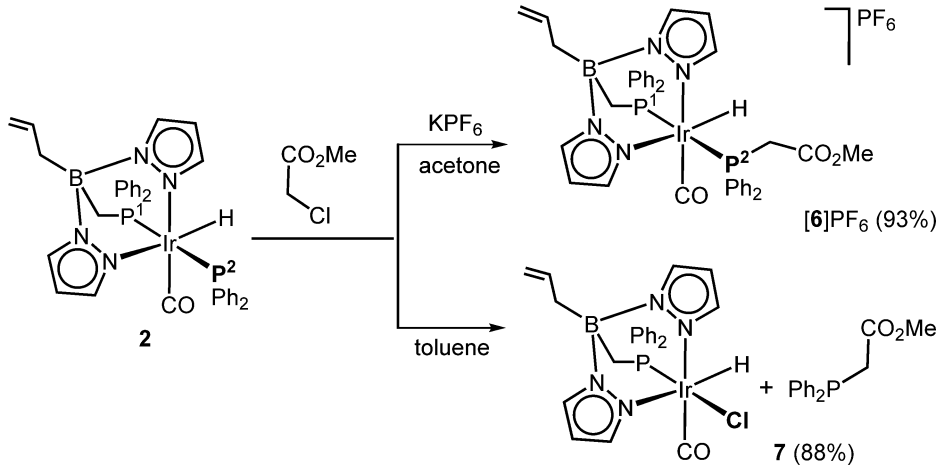

atom and iridium. Furthermore, following the intrinsic reaction coordinate of **TS1** in two directions showed that the transition state is directly connected with the complexes **A**-*SP* and **2**.

Reactions of 2 with Electrophiles. The nucleophilic character of the phosphanido ligand of complex **2** was evidenced from its reactions with electrophiles, such as H^+ and Me^+, in good agreement with the HOMO of complex **2** being essentially the phosphanido lone-pair (Figure 3). Both reactions were found to occur immediately to produce the white cationic complexes $[Ir(ABPN_2)(CO)(H)(PEPh_2)]^+$ (E = H, $[3]^+$; Me, $[4]^+$, Scheme 3). Quaternization of the parent phosphanido ligand in **2** results in a considerable enlargement of the $^2J_{P,P}$ coupling constant, from 97 Hz in **2** to ca. 310 Hz in complexes $[3]^+$ and $[4]^+$. This behavior has been systematically observed for the rest of the complexes reported here.

Oxygen also reacts with complex **2**, although the reaction was found to be slow, requiring around 12 h to reach completion. The product was identified as $[Ir(ABPN_2)(CO)(H)(POPh_2)]$ (**5**), where some reduction of the electronic density on the iridium atom in **5** was detected by an increase of the ν(CO) frequency from 2023 cm^{-1} in complex **2** to 2053 cm^{-1} in **5**.

Organic chlorides such as methyl chloroacetate ($ClCH_2CO_2Me$) also react with the phosphanido ligand at P2 in complex **2** (Scheme 4), and the outcome of the reaction was found to be very sensitive to the reaction conditions. Thus, if the reaction is carried out in acetone in the presence of stoichiometric amounts of KPF_6, the cationic complex $[Ir(ABPN_2)(CO)(H)(PPh_2CH_2CO_2Me)][PF_6]$ ($[6]PF_6$) was isolated after workup. Formation of the new P−C bond was confirmed through an $^1H,^{31}P$-hmbc NMR experiment where the expected correlation peaks between the CH_2 protons of the coordinated phosphane, Ir−$P^2Ph_2CH_2CO_2Me$, and P^2 were observed.

If the reaction is performed in less polar solvents such as benzene or toluene and in the absence of KPF_6, the products were found to be the neutral hydride chloride complex $[Ir(ABPN_2)(CO)(Cl)(H)]$ (**7**) and the free phosphane, $PPh_2CH_2CO_2Me$. In this case, the overall reaction involves the formal replacement of the functionalized phosphane by the chloride, an unexpected reaction because phosphanes are typically strongly bound to iridium. Moreover, dissociation of the phosphane is clearly evidenced by the observation of the hydride ligand in **7** as a doublet instead of a doublet of doublets (as observed for $[6]^+$). Furthermore, the free phosphane $PPh_2CH_2CO_2Me$ was easily identified from a singlet at δ = −16.5 ppm in the $^{31}P\{^1H\}$ NMR spectrum.[31] In addition, and according to its formula, complex **7** was independently prepared by reacting complex **2** with dry HCl in a 1:2 molar ratio. Its molecular structure is shown in Figure 6. The iridium atom in **7** shows an octahedral environment bound to the tripodal ligand and to the carbonyl, hydride, and chloride ligands, the latter being placed *trans* to the phosphorus atom. As expected, the strong *trans* influence of the hydride ligand is reflected in a longer Ir−N3 bond distance as compared to the Ir−N1 bond (Figure 6).

The cationic complex $[Ir(ABPN_2)(CO)(H)(PPh_2CH_2CO_2Me)][PF_6]$ ($[6]PF_6$) remains unaltered in solution, but in the presence of PPNCl (PPN = bis(triphenylphosphane)iminium) evolves cleanly and quantitatively to $[Ir(ABPN_2)(CO)(Cl)(H)]$ (**7**) and $PPh_2CH_2CO_2Me$. As such, we could assume that the first intermediate in the reaction of **2** with $ClCH_2CO_2Me$ in benzene is $[Ir(ABPN_2)$-

DOI: 10.1021/acs.inorgchem.5b02301
Inorg. Chem. 2016, 55, 828−839

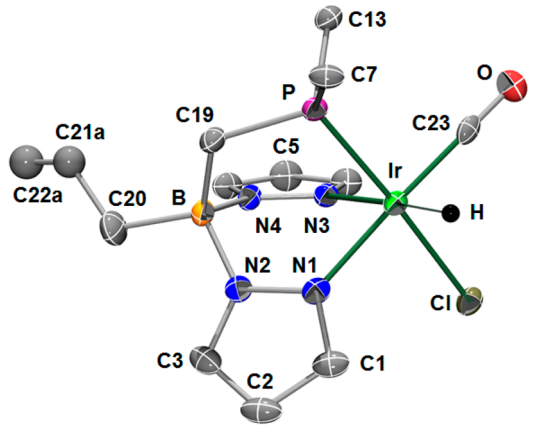

Figure 6. Molecular structure (ORTEP at the 50% level) of complex **7**. H atoms and the solvent of crystallization have been removed, and only the C^{ipso} atoms of the phenyl groups are shown for clarity. Selected bond distances (Å) and angles (deg): Ir–P, 2.273(1); Ir–N1, 2.074(3); Ir–N3, 2.159(3); Ir–C23, 1.854(5); Ir–H, 1.573(10); Ir–Cl, 2.421(1); C23–O, 1.139(5); P–Ir–Cl, 176.17(4); N1–Ir–C23, 177.07(15); N3–Ir–H, 177.7(15).

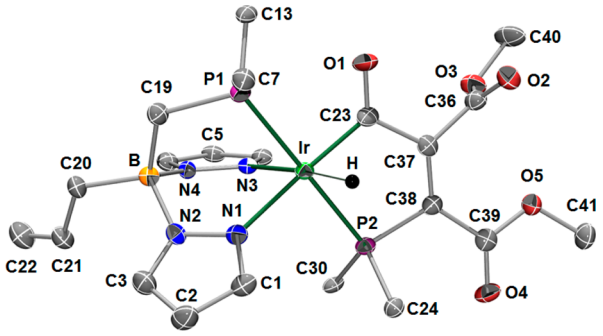

Figure 7. Molecular structure (ORTEP at the 50% level) of complex **8**. H atoms and the solvent of crystallization have been removed, and only the C^{ipso} atoms of the phenyl groups are shown for clarity. Selected bond distances (Å) and angles (deg): Ir–P1, 2.3473(13); Ir–P2, 2.2722(13); Ir–N1, 2.147(4); Ir–N3, 2.141(4); Ir–C23, 1.985(5); Ir–H, 1.569(10); C23–O1, 1.232(6); C23–C37, 1.547(7); C37–C38, 1.336(7); P2–C38, 1.822(5); P1–Ir–P2, 176.18(5); N1–Ir–C23, 177.48(19); N3–Ir–H, 174.2(19); Ir–P2–C38, 103.22(16); P2–C38–C37, 113.1(4); C38–C37–C23, 120.2(4); C37–C23–Ir, 117.8(3).

$(CO)(H)(PPh_2CH_2CO_2Me)]Cl$ ([**6**]Cl). However, on monitoring this reaction in C_6D_6 by NMR, the neutral species $[Ir(\kappa^2\text{-}ABPN_2)(CO)(Cl)(H)(PPh_2CH_2CO_2Me)]$ was observed instead (see the Supporting Information). Moreover, this species was found to be in a chemical equilibrium with the free phosphane and **7**. Therefore, coordination of chloride to iridium in ([**6**]Cl), induced by the low polarity of the solvent, seems to be the driving force to give complex **7** and $PPh_2CH_2CO_2Me$. All attempts to remove HCl from **7** to close a hypothetical catalytic cycle for the synthesis of functionalized phosphanes failed, and **7** was recovered after treating it with bases such as NEt_3 or KO^tBu in dichlorometane.

Reactions of 2 with Alkynes and Alkenes. The high nucleophilicity of the phosphanido group also promotes the engagement of complex **2** in P–C coupling reactions with activated alkynes and alkenes. Thus, reaction of **2** with $MeO_2CC{\equiv}CCO_2Me$ (dmad) gives rise to $[Ir(ABPN_2)(H)\{PPh_2\text{–}C(CO_2Me){=}C(CO_2Me)\text{–}CO\}]$ (**8**), which contains the new iridacyclophosphapentenone fragment shown in Scheme 5. Complex **8** was isolated as a white crystalline solid, and its molecular structure is shown in Figure 7.

As deduced from Figure 7, complex **8** retains the stereochemistry observed in phosphanido complex **2**, where the tripodal ligand is coordinated in a *facial* manner. The octahedral arrangement around iridium is completed by the hydride ligand and the five-membered iridacycle bound to iridium through P2 (*trans* to the phosphane arm of the scorpionate) and the ketonic carbonyl group.

The P2 atom displays the typical tetrahedral geometry expected for a phosphane type ligand, and, accordingly, a significant decrease in the Ir–P2 bond length is observed on going from **2** to **8**, which is expected on going from a (formal) covalent P–Ir bond to a dative P → Ir bond (vide infra). The five-membered iridacycle "Ir–P2–C37–C36–C35" is strictly planar, with the maximum deviation from the best plane being 0.028 Å. The C23–C37 and C37–C38 bond distances are appropriate for single and double carbon–carbon bonds, respectively (Figure 7), and comparable to related metallacyclophosphapentenone complexes of iron, molybdenum, or tungsten.[32] In good agreement, the angles around C37 and C38 of the incorporated alkyne fit with that expected for a sp^2 hybridization, reflecting clearly the formation of an olefin as a result of the formal cycloaddition process. Spectroscopic data of complex **8** in solution reflect accurately the structure observed in the solid state. Thus, the ketonic carbonyl group in the iridacycle was detected in the IR spectrum by a strong band at 1729 cm^{-1}, and, accordingly, it was low-field shifted from 170.4 (in **2**) to 207.0 ppm (in **8**) in the $^{13}C\{^1H\}$ NMR spectrum.

The most plausible mechanism involves a two-step process with the initial formation of the zwitterion **B** formed by nucleophilic attack of the phosphanido lone pair of **2** to the C≡C triple bond (Scheme 6), followed by attack on the

Scheme 5. Reaction of $[Ir(ABPN_2)(CO)(H)(PPh_2)]$ (2) with dmad ($MeO_2CC{\equiv}CCO_2Me$) To Give Complex 8

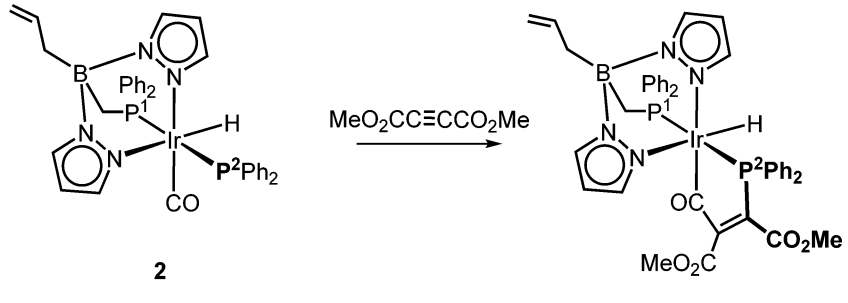

DOI: 10.1021/acs.inorgchem.5b02301
Inorg. Chem. 2016, 55, 828–839

Scheme 6. Plausible Mechanism for the Synthesis of Complex 8 from the Reaction of 2 with dmad[a]

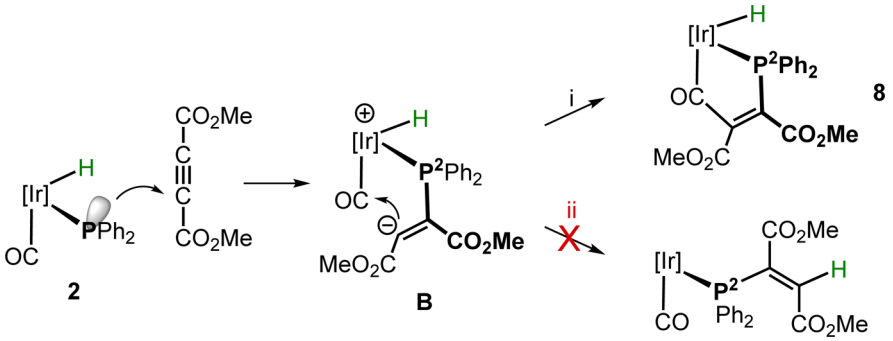

[a][Ir] = [Ir(ABPN$_2$)]. Path ii was not observed.

Scheme 7. Reaction of [Ir(ABPN$_2$)(CO)(H)(PPh$_2$)] (2) with Methyl Propiolate (HC≡CCO$_2$Me) To Give Complexes 9 and 10

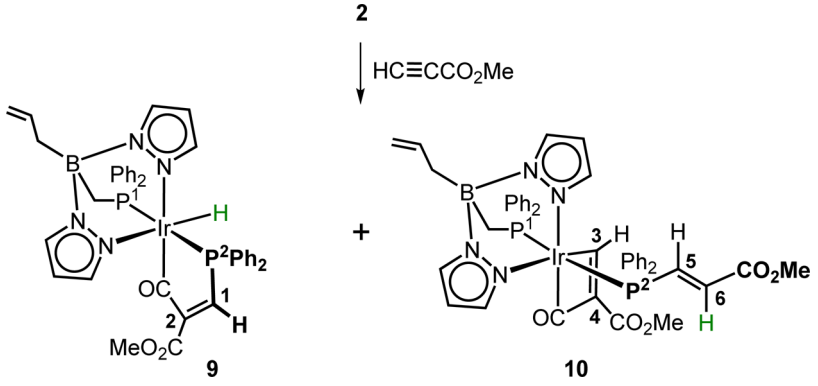

resulting carbanion to the terminal carbonyl group, as previously suggested for carbonyl complexes with terminal phosphanide,[32] thiolate,[33] iminophosphorane,[34] hydroxo,[35] or amido ligands.[36] Moreover, because complex **2** also contains a hydride ligand, abstraction of this hydrogen by the carbanion to give the iridium(I) derivative [Ir(ABPN$_2$)(CO){PPh$_2$−C(CO$_2$Me)=CH(CO$_2$Me)}] could also be considered (path ii, Scheme 6), but no evidence for such a complex was obtained when monitoring the reaction by NMR. The alternative pathway involving a concerted cycloaddition process could be also considered, but we were thus far unable to locate such a concerted transition state with DFT. Furthermore, the products obtained upon reaction of **2** with a monosubstituted alkyne are indicative of a stepwise process (see discussion below and Scheme 7).

The related monosubstituted alkyne methyl propiolate (HC≡CCO$_2$Me) also reacts with the phosphanide complex **2** leading to a mixture of complexes **9** and **10** (Scheme 7) in a variable ratio depending on the amount of the alkyne added. Thus, addition of 1.5 mol equiv of HC≡CCO$_2$Me to **2** produces an almost equimolar mixture of both products, while a ratio of 32:67 **9**:**10** can be obtained by adding the alkyne in excess (5 mol equiv).

Complex **9** was identified as the iridacyclophosphapentenone compound [Ir(ABPN$_2$)(H){PPh$_2$−CH=C(CO$_2$Me)−CO}] by its spectroscopic data, similar to those corresponding to complex **8** (see the Supporting Information). Moreover, complex **9** is indeed the isomer expected for a Michael-type nucleophilic attack of the phosphanide to the alkyne.

The second product from the reaction was identified as [Ir(ABPN$_2$){CH=C(CO$_2$Me)−CO}{PPh$_2$−CH=CH(CO$_2$Me)}] (**10**), having an iridacyclobutenone fragment and the functionalized phosphane Ph$_2$P−CH=CH(CO$_2$Me) (Scheme 7) according to its spectroscopic data (see the Supporting Information). The iridacyclobutenone fragment was supported by the observation of the Ir−C^{3}H= proton at very low field (δ = 9.46 ppm) in the ^{1}H NMR spectrum, while the high field shift of the ketonic Ir−CO carbon up to to δ = 177.3 ppm can be attributed to the four-membered nature of the iridacycle in complex **10**.

According to Scheme 6, complex **9** is the expected result from path i, while formation of complex **10** would require path ii, to give [Ir(ABPN$_2$)(CO){PPh$_2$−CH=CH(CO$_2$Me)}] in this case, followed by alkyne coordination and CO insertion into the metallacyclopropene ring. While a concerted [2+2] cycloaddition reaction cannot be fully disregarded, it seems less likely considering the product mixture obtained in the reaction described in Scheme 7. Furthermore, we were thus far unable to locate such a concerted transition state with DFT.

In any case, this was a quite unexpected reaction because isolated mononuclear metallacyclobutenone complexes are very rare, despite the interest of such type of complexes in metal-centered alkyne−carbonyl coupling reactions.[37] Reported examples include complexes of ruthenium,[38] iron,[39] rhenium,[40] and iridium[41] obtained from reactions of carbonyl compounds with activated alkynes and of platinum[42] and cobalt[43] coming from metal insertion into cyclopropenones.

To verify the participation of the iridium(I) species [Ir(ABPN$_2$)(CO){PPh$_2$−CH=CH(CO$_2$Me)}] in the formation of complex **10**, a model reaction between [{Ir(ABPN$_2$)(CO)}$_2$(μ-CO)] (**1**) and PPh$_2$Me (to generate the mononuclear complex [Ir(ABPN$_2$)(CO)(PPh$_2$Me)]) followed by the addition of 1 mol equiv of HC≡CCO$_2$Me was carried out. The overall reaction produces clean and quantitatively complex

DOI: 10.1021/acs.inorgchem.5b02301
Inorg. Chem. 2016, 55, 828−839

Scheme 8. Reaction of the Dinuclear Complex $[\{Ir(ABPN_2)(CO)\}_2(\mu\text{-}CO)]$ (1) with Methyldiphenylphosphane and Then with Methyl Propiolate ($HC{\equiv}CCO_2Me$) To Give Complex 11

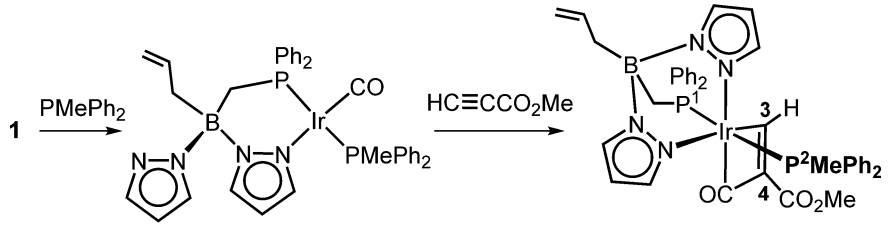

$[Ir(ABPN_2)\{CH{=}C(CO_2Me){-}CO\}(PPh_2Me)]$ (**11**), which was isolated as a white crystalline solid in 94% yield (Scheme 8). Spectroscopic data of **11** were those expected for a complex having an iridacyclobutenone fragment (see the Supporting Information).

The related alkynes HC≡CH, HC≡CPh, and PhC≡CPh, having less electrophilic carbons than $HC{\equiv}CCO_2Me$ and $MeO_2CC{\equiv}CCO_2Me$, do not react with complex **2**, which supports the mechanism depicted in Scheme 6 starting with the nucleophilic attack of the phosphanido ligand.

Activated olefins such as dimethyl maleate (*cis*-$MeO_2CCH{=}CHCO_2Me$) also react with the phosphanide complex $[Ir(ABPN_2)(CO)(H)(PPh_2)]$ (**2**) to give the complex $[Ir(ABPN_2)(H)\{PPh_2{-}CH(CO_2Me){-}CH(CO_2Me){-}CO\}]$ (**12**, Scheme 9), the aliphatic version of the iridacycle above-described for complexes **8** and **9**. Because complex **12** contains three stereogenic centers, the iridium atom and the two carbons of the iridacycle, four pairs of enantiomers could be expected a priori to result. Indeed, if the reaction is carried out at −30 °C, some of them can be observed, but they evolve to the thermodynamic pair of enantiomers on raising the temperature, which corresponds to the isolated product.

Scheme 9. Reaction of $[Ir(ABPN_2)(CO)(H)(PPh_2)]$ (2) with Either *cis*- or *trans*-$MeO_2CCH{=}CHCO_2Me$ To Give Complex 12[a]

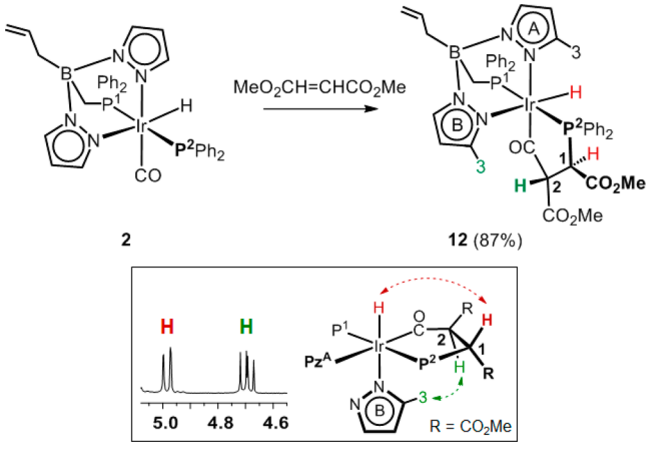

[a]The inset shows a selected region of the ^1H NMR spectrum of **12**, while the arrows indicate the close proximity of some protons according to selnOe NMR spectra.

The methylene protons of the new formed iridacyclophosphapentanone were observed at δ = 4.98 ($J_{H,H}$ = 13.2 Hz, $^2J_{H,P}$ = 1.4 Hz) and 4.69 ($J_{H,H}$ = 13.2 Hz, $^3J_{H,P}$ = 10.9 Hz) ppm (in red and green, respectively, in Scheme 9). The different values for the $J_{H,P}$ coupling constants allowed the assignment of both protons because $^3J_{H,P}$ is expected to be larger than $^2J_{H,P}$. Moreover, the large $J_{H,H}$ coupling constant suggests both protons to be in an antiperiplanar conformation (torsion angle around 180°), while selective selnOe experiments allowed one to unambiguously establish the stereochemistry of **12** (see the Supporting Information).

Complex **12** was also the product from the reaction between **2** and dimethyl fumarate (*trans*-$MeO_2CCH{=}CHCO_2Me$) as observed by "in situ" NMR experiments, which otherwise confirm the thermodynamic control of both reactions. In this case, monitoring the reaction by NMR revealed a more complicated mechanism than that expected from the stepwise pathway exemplified in Scheme 6 for the alkynes case. Four major compounds were observed: complex **12** and one of its isomers (**12′**), the free phosphane, $PPh_2CH(CO_2Me){-}CH_2(CO_2Me)$, and a new species having broad resonances that have been attributed to the iridium(I) complex $[Ir(ABPN_2)(CO)(PPh_2R)]$ (R = $CH(CO_2Me)CH_2(CO_2Me)$, **D**) (Figure 8). This mixture cleanly evolves to complex **12**, along with small amounts of the free phosphane, $PPh_2CH(CO_2Me){-}CH_2(CO_2Me)$, overnight (see the Supporting Information).

Participation of the iridium(I) complex $[Ir(ABPN_2)(CO){-}(PPh_2R)]$ (R = $CH(CO_2Me)CH_2(CO_2Me)$, **D**) in the course of the reaction was confirmed by the reaction between the dinuclear complex $[\{Ir(ABPN_2)(CO)\}_2(\mu\text{-}CO)]$ (**1**) and the phosphane $PPh_2CH(CO_2Me)CH_2(CO_2Me)$, which produces a $^{31}P\{^1H\}$ NMR spectrum after 5 min of reaction (see the Supporting Information), similar to that observed in the

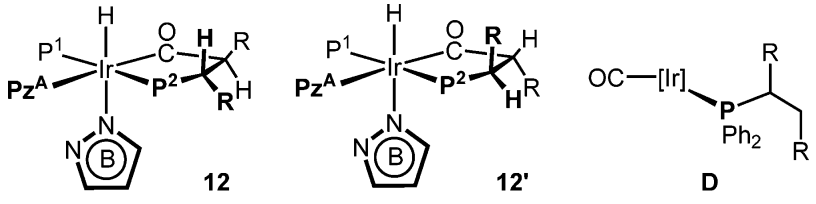

Figure 8. Complexes detected on monitoring the reaction of complex **2** with dimethyl fumarate. R = CO_2Me.

DOI: 10.1021/acs.inorgchem.5b02301
Inorg. Chem. 2016, 55, 828−839

Scheme 10. Transformation of [Ir(ABPN$_2$)(CO)(PPh$_2$R)] (R = CH(CO$_2$Me)CH$_2$(CO$_2$Me), D) in Complex 12 and a Plausible Way for the Isomerization of 12′ into 12 through the Enol Intermediates E1 and E2

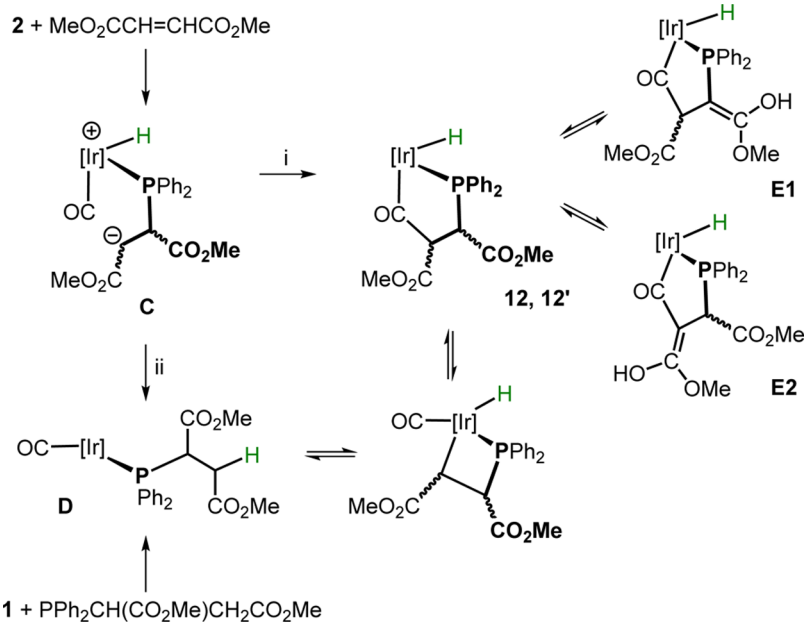

reaction of **2** with dimethyl fumarate. This mixture evolved to complex **12** as expected.

Understanding the overall reactions is not obvious. Assuming a two-step mechanism similar to that shown in Scheme 6 for the alkynes case, complexes **12** and **12′** would come from the nucleophilic attack of the phosphanido in **2** to one face (or the other) of dimethyl fumarate to give the carbanion **C** (Scheme 10) followed by the attack of the resulting carbanion to the terminal carbonyl group (path i). The alternative proton migration from the iridium to the carbanion (path ii) would produce the iridium(I) complex **D**. Starting from **D**, the formation of **12** and **12′** would require the concurrence of an oxidative-addition reaction of one the methylenic protons in the −CH$_2$(CO$_2$Me) group and the migratory insertion of the carbonyl group into the Ir−C bond (Scheme 10). This migration generates a more favorable, less strained five-membered metallacycle and has been previously observed in iridium chemistry.[44]

Isomerization of complex **12′** into **12** could take place through the participation of the enol-type intermediates **E1** and **E2** (Scheme 10). Indeed, on heating (40 °C) a solution of complex **12** in the presence of a small amount of D$_2$O, deuteration of both methylenic protons was observed. Figure 9 shows a couple of spectra at the beginning of the reaction (bottom trace) and after 17 h at 40 °C in the presence of 5 mol equiv of D$_2$O (top trace), where a similar decrease in the intensity of the signal corresponding to the methylenic protons is clearly observed. The remaining resonances correspond to the complexes [Ir(ABPN$_2$)(X){PPh$_2$−CX(CO$_2$Me)−CY(CO$_2$Me)−CO}] (X = H, Y = D; X= D, Y = D). Although enols from esters are quite uncommon, its participation provides the simplest explanation to account for the experimental observations.

Moreover, Figure 9 also shows deuteration at the hydride position suggesting that the equilibrium between **12** and **D** or, alternatively, between **12** and **2** and MeO$_2$CH═CHCO$_2$Me is also operative (Scheme 10). The latter possibility has been confirmed from the reaction between **2** and dimethyl maleate in

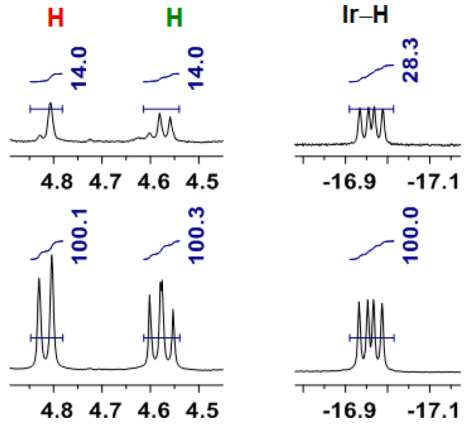

Figure 9. Selected regions of the ^{1}H NMR spectra of complex **12** (bottom) and after 17 h at 40 °C in the presence of 5 mol equiv of D$_2$O (top).

a ratio 1:5, which produces complex **12** and dimethyl fumarate after 3 days. This olefin isomerization gives support to the proposed double retro-fragmentation reaction in **12**, associated with the decoordination of the olefin. Such type of isomerizations through metallacyclopentanones has been previously observed in cyclopentamethyl iron complexes.[32b] Finally, considering the values of the integrals in Figure 9, it is clear that the equilibria involving the methylenic protons show a lower activation barrier than the equilibria involving the hydride ligand.

SUMMARY AND CONCLUSIONS

In this Article, we showcase the ability of an iridium complex to react with a secondary phosphane to afford an iridium(III) compound (**2**) with a terminal phosphanido ligand. This rare compound results formally from the oxidative addition of a P−H bond to iridium(I). The reactivity of the phosphanido complex is governed by the nucleophilicity of the phosphanido phosphorus atom. Thus, simple electrophiles (H$^+$, Me$^+$, O$_2$)

DOI: 10.1021/acs.inorgchem.5b02301
Inorg. Chem. 2016, 55, 828−839

directly attack the phosphorus atom leading to the formation of P−H, P−C, and P═O bonds, respectively. In the same fashion, the reaction with ethyl chloroacetate in the presence of KPF_6 gives the cation with a functionalized phosphane $[Ir(ABPN_2)(CO)(H)(PPh_2CH_2CO_2Me)]^+$ by a P−C coupling reaction, while in the absence of the salt the free phosphane $PPh_2CH_2CO_2Me$ results along with the hydrido complex $[Ir(ABPN_2)(CO)(Cl)(H)]$. The terminal phosphanido complex is appropriate to undergo P−C coupling reactions with activated unsaturated hydrocarbons. Nonetheless, the presence of a nucleophilic phosphorus atom and a terminal carbonyl ligand in the complex induces cycloaddition processes that involve the concomitant formation of P−C and C−C bonds, as illustrated by the synthesis of iridacyclophosphapentenone complexes $[Ir(ABPN_2)(H)\{PPh_2-CR{=}C(CO_2Me)-CO\}]$ (R = CO_2Me, H) from reactions of **2** with dimethyl acetylenedicarboxylate and methyl propiolate, respectively. A parallel reaction in the second case also affords a rare iridacyclobutenone complex $[Ir(ABPN_2)\{CH{=}C(CO_2Me)-CO\}\{PPh_2-CH{=}CH(CO_2Me)\}]$ by alkyne coordination and CO insertion into the metallacyclopropene ring. Activated alkenes such as dimethyl maleate and dimethyl fumarate also reacted with **2** to form eventually the same iridacyclophosphapentanone complex $[Ir(ABPN_2)(H)\{PPh_2-CH(CO_2Me)-CH(CO_2Me)-CO\}]$, the thermodynamic product of both reactions. Deuterium exchange of the methylenic and hydride protons in the presence of D_2O as well as isomerization of dimethyl maleate into dimethyl fumarate suggest that several equilibria involving enol-type species and double-retrofragmentation steps are involved in the mechanism.

EXPERIMENTAL SECTION

General Methods. All procedures were performed under an argon atmosphere, using standard Schlenk techniques. Solvents were dried and distilled under argon before use by standard methods.[45] Carbon, hydrogen, and nitrogen analyses were carried out with a PerkinElmer 2400 CHNS/O microanalyzer. High-resolution electrospray mass spectra were acquired on a Bruker Microtof-Q (ESI$^+$). NMR spectra were recorded on Bruker AV 300, AV 400, and AV 500 spectrometers operating at 300.13, 400.13, and 500.13 MHz, respectively, for ^{1}H. Chemical shifts are reported in ppm and referenced to $SiMe_4$, using the internal signal of the deuterated solvent (^{1}H and ^{13}C) and external H_3PO_4 (^{31}P). IR spectra in solution were recorded with a Nicolet 550 spectrophotometer using NaCl cells, while IR spectra of solid samples were recorded with a PerkinElmer 100 FT-IR spectrometer (4000−400 cm^{-1}) equipped with an ATR (attenuated total reflectance). Conductivities were measured in acetone solutions (5.0×10^{-4} M) using a Philips PW 9501/01 conductimeter. Recorded values for complexes [**3**]BF_4, [**4**]OTf, and [**6**]PF_6 were found to be in agreement with 1:1 electrolytes (54−79 Ω^{-1} cm^2 mol^{-1}). The complex $[\{Ir(ABPN_2)(CO)\}_2(\mu\text{-}CO)]$[25a] (**1**) was prepared according to the literature description. All other chemicals are commercially available and were used without further purification.

*Synthesis of the Complexes: [Ir(ABPN$_2$)(CO)(H)(PPh$_2$)] (**2**).* Diphenylphosphane (28.1 μL, 0.16 mmol) was added via microsyringe to a yellow solution of **1** (100.4 mg, 0.08 mmol) in THF (5 mL). Evolution of gaseous carbon monoxide was observed. After 30 min of stirring, the solution was concentrated to ca. 0.5 mL, and then hexane (5 mL) was added. The pale-yellow solid that precipitated was filtered out, washed with hexane (2 × 5 mL), and dried under vacuum. Colorless microcrystals suitable for X-ray diffraction studies were obtained by layering a solution of **2** in THF with hexane. Yield: 117.4 mg (92%). IR (ATR): ν(Ir−H)/cm^{-1} 2233 (w), ν(CO)/cm^{-1} 2023 (s). MS (MALDI-TOF$^+$): *m*/*z* (%) 793.4 (100) [M$^+$ + H], 765.4 (40) [M$^+$ + H − CO]. Anal. Calcd for $C_{35}H_{34}BIrN_4OP_2$: C, 53.10; H, 4.33; N, 7.08. Found: C, 53.26; H, 4.56; N, 6.88. For NMR data, see the Supporting Information.

*[Ir(ABPN$_2$)(CO)(D)(PPh$_2$)] (**2**-d$_1$).* A NMR tube was loaded with **1** (15 mg, 0.01 mmol) and dissolved in benzene (0.5 mL). Deuterated diphenylphosphane (D-PPh$_2$, 4 μL, 0.02 mmol) was then added to the solution. ^{2}D NMR (400 MHz, C_6H_6, 25 °C): δ −15.09 (br, 1H; Ir−D).

*[Ir(ABPN$_2$)(CO)(H)(PHPh$_2$)][BF$_4$] ([**3**]BF$_4$).* $HBF_4{\cdot}O(CH_2CH_3)_2$ (21 μL, 0.15 mmol) was added to a suspension of **2** (121.7 mg, 0.15 mmol) in diethyl ether (5 mL), giving rise immediately to the formation of a white precipitate. After the suspension was stirred for 1 h, the solid was filtered off, washed with cold diethyl ether (2 × 4 mL), and dried out by vacuum. Yield: 94.1 mg (70%). IR (ATR): ν(Ir−H)/cm^{-1} 2185 (w), ν(CO)/cm^{-1} 2065 (s). MS (MALDI-TOF$^+$): *m*/*z* (%) 793.2 (100) [M − H], 607.2 (25) [M − H − HPPh$_2$], 577.0 (20) [M − 2H − HPPh$_2$ − CO]. Anal. Calcd for $C_{35}H_{35}B_2IrN_4OP_2$: C, 52.32; H, 4.39; N, 6.97. Found: C, 52.58; H, 4.55; N, 6.72. Λ_M = 57.9 Ω^{-1} cm^2 mol^{-1} (acetone, 5.0×10^{-4} M). For NMR data, see the Supporting Information.

*[Ir(ABPN$_2$)(CO)(H)(PMePh$_2$)][OTf] ([**4**]OTf).* Complex **2** (136.2 mg, 0.17 mmol) was suspended in diethyl ether (5 mL), and then neat methyl triflate (19 μL, 0.17 mmol) was added via microsyringe. The resulting white suspension was stirred for 30 min, and the solid was isolated by filtration, washed with diethyl ether, and then dried under vacuum. Yield: 100.5 mg (60%). IR (ATR): ν(Ir−H)/cm^{-1} 2201 (w), ν(CO)/cm^{-1} 2062 (s). MS (MALDI-TOF$^+$): *m*/*z* (%) 807.2 (30) [M$^+$], 779.2 (35) [M$^+$ − CO], 607.2 (100) [M$^+$ − CH_3PPh_2]. Anal. Calcd for $C_{37}H_{37}BF_3IrN_4O_5P_2S$: C, 45.73; H, 3.85; N, 5.77. Found: C, 45.72; H, 3.69; N, 5.61. Λ_M = 79.1 Ω^{-1} cm^2 mol^{-1} (acetone, 5.0×10^{-4} M). For NMR data, see the Supporting Information.

*[Ir(ABPN$_2$)(CO)(H)(POPh$_2$)] (**5**).* A solution of **2** (80.0 mg, 0.10 mmol) in THF (4 mL) was shaken under an oxygen atmosphere for 12 h. The solvent was removed and the residue was stirred with hexane (5 mL) to render a white solid, which was filtered off, washed with hexane (3 × 5 mL), and dried under vacuum. Yield: 78.2 mg (95%). IR (C_6D_6): ν(Ir−H)/cm^{-1} 2184 (w), ν(CO)/cm^{-1} 2053 (s), ν(P═O)/cm^{-1} 1210. MS (MALDI-TOF$^+$): *m*/*z* (%) 808.2 (100) [M$^+$], 806.2 (60) [M$^+$ − 2H]. Anal. Calcd for $C_{35}H_{34}BIrN_4O_2P_2$: C, 52.05; H, 4.23; N, 6.94. Found: C, 51.74; H, 4.13; N, 6.98. For NMR data, see the Supporting Information.

*[Ir(ABPN$_2$)(CO)(H)(PPh$_2$CH$_2$CO$_2$Me)][PF$_6$] ([**6**]PF$_6$).* To a solution of **2** (107.6 mg, 0.14 mmol) in acetone (8 mL) was added methyl chloroacetate (13.1 μL, 0.14 mmol) via microsyringe. The mixture was stirred for 30 s, and then KPF_6 (25.0 mg, 0.14 mmol) was added. The cloudy solution was stirred overnight at room temperature. The solvent was removed by vacuum, and dichloromethane (10 mL) was added. The cloudy solution was filtered out to eliminate the precipitated KCl, and the reaction was evaporated to ca. 0.5 mL. Addition of diethyl ether (5 mL) yielded a white solid, which was filtered off, and then it was vacuum-dried. Yield: 127.8 mg (93%). IR (CD_2Cl_2): ν(Ir−H)/cm^{-1} 2183 (w), ν(CO)/cm^{-1} 2050 (s), ν(C═O)/cm^{-1} 1729 (s, br), ν(C−O)/cm^{-1} 1101 and 1072 (s), ν(PF_6)/cm^{-1} 832 and 741. MS (MALDI-TOF$^+$): *m*/*z* (%) 865.2 (95) [M$^+$]. Anal. Calcd for $C_{38}H_{39}BF_6IrN_4O_3P_3$ (1009.68): C, 45.20; H, 3.89; N, 5.55. Found: C, 45.43; H, 3.84; N, 5.70. Λ_M = 54.1 Ω^{-1} cm^2 mol^{-1} (acetone, 5×10^{-4} M). For NMR data, see the Supporting Information.

*[Ir(ABPN$_2$)(CO)(Cl)(H)] (**7**).* Method A: To a colorless solution of **2** (103.6 mg, 0.13 mmol) in toluene (4 mL) was added methyl chloroacetate (13.8 μL, 0.16 mmol) in a slight excess (1:1.2) via microsyringe. The reaction mixture was stirred for 2 h at 50 °C, and the solution was then dried under vacuum, yielding an oily residue. Hexanes (5 mL) were added, affording a whitish solid that was isolated by filtration and dried by vacuum. The washing solution was collected and filtered through a pad of silica, and upon removal of the solvents the phosphane $PPh_2CH_2CO_2Me$ was obtained as an oily material (see below). Yield: 73.9 mg (88%). Method B: Complex **1** (97.0 mg, 0.08 mmol) was dissolved in diethyl ether (4 mL), and a solution of dry HCl in Et_2O (0.68 M, 0.23 mL) was added via microsyringe inducing the immediate precipitation of a white solid. Upon 30 min of stirring,

DOI: 10.1021/acs.inorgchem.5b02301
Inorg. Chem. 2016, 55, 828−839

the solid was isolated by filtration and then vacuum-dried. Yield: 92.5 mg (92%). IR (toluene): ν(Ir−H)/cm^{-1} 2189 (w), ν(CO)/cm^{-1} 2057 (s). MS (MALDI-TOF$^+$): m/z (%) 681.2 (25) [M$^+$ + K], 607.2 (100) [M$^+$ − Cl]. Anal. Calcd for $C_{23}H_{24}BClIrN_4OP$ (641.92): C, 43.03; H, 3.77; N, 8.73. Found: C, 43.40; H, 4.02; N, 8.40. For NMR data, see the Supporting Information.

$PPh_2CH_2CO_2Me$ was obtained as a byproduct from the formation of **7** as a colorless oil (method A). Yield: 26.9 mg (80%). ^{1}H NMR (500 MHz, C_6D_6, 25 °C): δ 7.40 (m, 4H; H^o PPh_2), 7.04 (m, 6H; H^{m+p} PPh_2), 3.19 (s, 3H; OCH_3), 2.94 (m br, 2H; CH_2P). ^{31}P{^{1}H} NMR (202 MHz, C_6D_6, 25 °C): δ −16.5 (br). ^{13}C{^{1}H} NMR (125 MHz, C_6D_6, 25 °C): δ 170.4 (d, $^2J_{C,P}$ = 8 Hz; CO), 136.3 (d, $^1J_{C,P}$ = 60 Hz; C^i PPh_2), 133.1 (d, $^2J_{C,P}$ = 20 Hz, 2C; C^o PPh_2), 129.1 (2C; C^p PPh_2), 128.8 (m, 2C; C^m PPh_2), 51.4 (OCH_3), 35.2 (d, $^1J_{C,P}$ = 21 Hz; CH_2P).[31]

*Detection of [Ir(ABPN$_2$)(CO)(Cl)(H)(PPh$_2$CH$_2$CO$_2$Me)] (**B**).* To a NMR tube loaded with **2** (14.2 mg, 0.018 mmol) and dissolved in C_6D_6 (0.5 mL) was added methyl chloroacetate (1.6 μL, 0.018 mmol) via microsyringe, and the reaction was left at room temperature for 2 h. Spectroscopic measurements revealed consumption of **2**, and formation in solution of **6**, $Ph_2PCH_2CO_2Me$, and a new complex, identified as **B**. For NMR data, see the Supporting Information.

*[Ir(ABPN$_2$)(H){PPh$_2$−C(CO$_2$Me)═C(CO$_2$Me)−CO}] (**8**).* To a solution of **2** (102.7 mg, 0.13 mmol) in THF (5 mL) was added dimethyl acetylenedicarboxylate (dmad) (16 μL, 0.13 mmol), causing an instant darkening of the solution. After 1 h of stirring, the solution was evaporated to ca. 0.5 mL, and then hexane (5 mL) was added causing the precipitation of a brown solid, which was filtered off, washed with hexane (2 × 5 mL), and dried by vacuum yielding a pale brown solid. Slow diffusion of cold hexanes into a solution of **8** and THF yielded brown microcrystals suitable for X-ray diffraction studies. Yield: 120.6 mg (91%).IR (ATR): ν(Ir−H)/cm^{-1} 2162 (w), ν(C═O)/cm^{-1} 1729 (s, br), ν(C−O)/cm^{-1} 1243 (m, br). MS (MALDI-TOF$^+$): m/z (%) 957.3 (50) [M$^+$ + Na], 935.3 (38) [M$^+$ + H], 933.3 (38) [M$^+$ − H], 607.3 (45) [M$^+$ − dma − PPh_2 + H]. Anal. Calcd for $C_{41}H_{40}BIrN_4O_5P_2$: C, 52.74; H, 4.32; N, 6.00. Found: C, 53.13; H, 4.22; N, 5.84. For NMR data, see the Supporting Information.

Reaction of 2 with Methyl Propiolate. To a solution of **2** (28.6 mg, 0.04 mmol) in [D$_8$]toluene (0.5 mL) was added methyl propiolate (3 μL, 0.04 mmol), and the solution became yellow. NMR measurements showed total conversion of **2** into **9** and **10** in an 11:9 ratio (NMR integration). In a parallel experiment, methyl propiolate (6 μL, 0.07 mmol) was added in excess (5:1) to a [D$_8$]toluene (0.5 mL) solution of **2** (10.8 mg, 0.014 mmol). Full conversion of **2** into **9** and **10** was observed via NMR, in a 1:2 ratio (NMR integration). See the Supporting Information for detailed NMR data.

*[Ir(ABPN$_2$){CH═C(CO$_2$Me)−CO}(PPh$_2$Me)] (**11**).* To a solution of **1** (90.8 mg, 0.07 mmol) in toluene (5 mL) was added methyl diphenylphosphane (27.6 μL, 0.15 mmol) to give a yellowish solution. After 1 min of stirring, methyl propiolate (12.2 μL, 0.15 mmol) was added via microsyringe, and the solution was then stirred at room temperature for 2 h. The solvent was removed under vacuum to give an orange residue that was treated with cold hexane yielding a yellow solid, which was filtered off and dried by vacuum. Yield: 122.4 mg (94%). IR (ATR): ν(C═O)/cm^{-1} 1704 (s, br), 1683 (s, br). MS (MALDI-TOF$^+$): m/z (%) 891.0 (38) [M$^+$ + H], 889.0 (42) [M$^+$ − H], 807.0 (100) [M$^+$ − $C_4H_4O_2$], 691.2 (59) [M$^+$ − PPh_2CH_3 + H], 607.0 (15) [M$^+$ − PPh_2CH_3 − $C_4H_4O_2$ + H]. Anal. Calcd for $C_{40}H_{40}BIrN_4O_3P_2$: C, 54.00; H, 4.53; N, 6.30. Found: C, 53.42; H, 4.08; N, 6.01. For NMR data, see the Supporting Information.

*[Ir(ABPN$_2$)(H){PPh$_2$−CH(CO$_2$Me)−CH(CO$_2$Me)−CO}] (**12**).* Method A: To a solution of **2** (104 mg, 0.13 mmol) in toluene (4 mL) was added dimethyl maleate (17 μL, 0.13 mmol) via microsyringe, and the resulting solution was stirred for 16 h. The solvent was then evaporated to ca. 0.5 mL, and hexanes were added affording a yellow solid, which was then filtered off and dried by vacuum. Yield: 105.7 mg (87%). Method B: Addition of solid dimethyl fumarate (4 mg, 0.03 mmol) to a yellow solution of **2** (22.4 mg, 0.03 mmol) in C_6D_6 (0.5 mL) into a NMR tube led to a clear yellow solution. NMR measurements after 28 h showed quantitative conversion to complex **12**. IR (C_6D_6): ν(Ir−H)/cm^{-1} 2173 (w), ν(C═O)/cm^{-1} 1741 (s, br), ν(C−O)/cm^{-1} 1209 (m, br). MS (MALDI-TOF$^+$): m/z (%) 937.3, (30) [M$^+$ + H], 792.2 (1) [M$^+$ − $C_6H_8O_4$]. Anal Calcd for $C_{41}H_{42}BN_4IrO_5P_2$: C, 52.62; H, 4.52; N, 5.99. Found: C, 52.11; H, 4.45; N, 5.62. For NMR data, see the Supporting Information.

DFT Geometry Optimizations. Geometry optimizations were carried out with the Turbomole program package[46] coupled to the PQS Baker optimizer[47] via the BOpt package,[48] at the DFT/b3-lyp[49] level. We used the def2-TZVP basis set[50] (small-core pseudopotentials on Ir[51]) for the geometry optimizations. Scalar relativistic effects were included implicitly through the use of the Ir ECPs. Minima (no imaginary frequencies) and the transition state (one imaginary frequency) were characterized by calculating the Hessian matrix. ZPE and gas-phase thermal corrections (entropy and enthalpy, 298 K, 1 bar) from these analyses were calculated. The nature of the transition state was confirmed by IRC calculations. The optimized geometries of all species are supplied as separate files in .pdb and.xyz format. Mayer[52] bond orders were calculated from the Turbomole output files using the AOMix program.[53]

X-ray Diffraction Studies on Complexes 2·0.5(C_6H_{14}), 7·0.4(C_6H_6), and 8·(C_7H_8). Intensity measurements were collected with a Smart Apex diffractometer, with graphite-monochromated Mo Kα radiation. A semiempirical absorption correction was applied to each data set, with the multiscan[54] methods. Selected crystallographic data can be found in the Supporting Information. The structures were solved by the Patterson method and refined by full-matrix least-squares, with the program SHELX2013[55] in the WINGX[56] package. The hydride ligands were found in residual electron density maps and refined free but with a restrained distance to the metal atom, with free isotropic displacement parameters for **2** and **8**, and a riding one for complex **7**.

■ ASSOCIATED CONTENT

Supporting Information

The Supporting Information is available free of charge on the ACS Publications website at DOI: 10.1021/acs.inorgchem.5b02301.

Selected crystallographic data, and selected NMR spectra for the complexes (PDF)

X-ray data for compounds 2·0.5(C_6H_{14}), 7·0.4(C_6H_6), and 8·(C_7H_8) (CIF)

X,Y,Z coordinates for DFT-calculated intermediates and transition states (XYZ)

■ AUTHOR INFORMATION

Corresponding Author

*E-mail: ctejel@unizar.es.

Notes

The authors declare no competing financial interest.

■ ACKNOWLEDGMENTS

The generous financial support from MICINN/FEDER (Project CTQ2011-22516) and MINECO/FEDER (Projects CTQ2012-35665 and CTQ2014-53033-P), Gobierno de Aragón/FSE (GA/FSE, Inorganic Molecular Architecture Group, E70), and NWO-CW (VICI project 016.122.613; B.d.B.) is gratefully acknowledged. A.L.S. thanks MEC for a fellowship.

■ REFERENCES

(1) (a) Hooper, T. N.; Huertos, M. A.; Jurca, T.; Pike, S. D.; Weller, A. S.; Manners, I. *Inorg. Chem.* **2014**, *53*, 3716−3729. (b) Huertos, M. A.; Weller, A. S. *Chem. Sci.* **2013**, *4*, 1881−1888. (c) Leitao, E. M.; Jurca, T.; Manners, I. *Nat. Chem.* **2013**, *5*, 817−829. (d) Waterman, R.

DOI: 10.1021/acs.inorgchem.5b02301
Inorg. Chem. 2016, 55, 828−839

Curr. Org. Chem. **2012**, *16*, 1313−1331. (e) Ghebreab, M. B.; Shalumova, T.; Tanski, J. M.; Waterman, R. *Polyhedron* **2010**, *29*, 42−45. (f) Waterman, R. *Dalton Trans.* **2009**, 18−26. (g) Greenberg, S.; Stephan, D. W. *Chem. Soc. Rev.* **2008**, *37*, 1482−1489. (h) Waterman, R. *Curr. Org. Chem.* **2008**, *12*, 1322−1339. (i) Glueck, D. S. *Dalton Trans.* **2008**, 5276−5286. (j) Clark, T. J.; Rodezno, J. M.; Clendenning, S. B.; Aouba, S.; Brodersen, P. M.; Lough, A. J.; Ruda, H. E.; Manners, I. *Chem. - Eur. J.* **2005**, *11*, 4526−4534. (k) Jaska, C. A.; Manners, I. *J. Am. Chem. Soc.* **2004**, *126*, 1334−1335. (l) Stephan, D. W. *Angew. Chem., Int. Ed.* **2000**, *39*, 314−329.

(2) (a) Waterman, R. *Chem. Soc. Rev.* **2013**, *42*, 5629−5641. (b) Jaska, C. A.; Bartole-Scott, A.; Manners, I. *Dalton Trans.* **2003**, 4015−4021. (c) Dorn, H.; Singh, R. A.; Massey, A.; Nelson, J. M.; Jaska, C. A.; Lough, A. J.; Manners, I. *J. Am. Chem. Soc.* **2000**, *122*, 6669−6678.

(3) (a) Greenhalgh, M. D.; Jones, A. S.; Thomas, S. P. *ChemCatChem* **2015**, *7*, 190−222. (b) Koshti, V.; Gaikwad, S.; Chikkali, S. H. *Coord. Chem. Rev.* **2014**, *265*, 52−73. (c) Sues, P. E.; Lough, A. J.; Morris, R. H. *J. Am. Chem. Soc.* **2014**, *136*, 4746−4760. and references therein. (d) Ghebreab, M. B.; Bange, C. A.; Waterman, R. *J. Am. Chem. Soc.* **2014**, *136*, 9240−9243. (e) Rosenberg, L. *ACS Catal.* **2013**, *3*, 2845−2855. (f) Glueck, D. S. *Top. Organomet. Chem.* **2010**, *31*, 65−100. (g) Glueck, D. S. *Chem. - Eur. J.* **2008**, *14*, 7108−7117. (i) Tanaka, M. *Top. Curr. Chem.* **2004**, *232*, 25−54.

(4) (a) Wauters, I.; Debrouwer, W.; Stevens, C. V. *Beilstein J. Org. Chem.* **2014**, *10*, 1064−1096. (b) Dillon, K. B.; Mathey, F.; Nixon, J. F. *From Organophosphorus to Phospha-organic Chemistry*; Wiley: Chichester, 1998.

(5) (a) Yang, X.-Y.; Gan, J. H.; Li, Y.; Pullarkat, S. A.; Leung, P.-H. *Dalton Trans.* **2015**, *44*, 1258−1263. (b) Yap, J. S. L.; Li, B. B.; Wong, J.; Li, Y.; Pullarkat, S. A.; Leung, P.-H. *Dalton Trans.* **2014**, *43*, 5777−5784. (c) Sabater, S.; Mata, J. A.; Peris, E. *Organometallics* **2013**, *32*, 1112−1120. (d) Chen, K.; Pullarkat, S. A.; Ma, M.; Li, Y.; Leung, P.-H. *Dalton Trans.* **2012**, *41*, 5391−5400. (e) Huang, Y.; Pullarkat, S. A.; Li, Y.; Leung, P.-H. *Inorg. Chem.* **2012**, *51*, 2533−2540. (f) Yang, M.-J.; Liu, Y.-J.; Gong, J.-F.; Song, M.-P. *Organometallics* **2011**, *30*, 3793−3803. (g) Huang, Y.; Pullarkat, S. A.; Li, Y.; Leung, P.-H. *Chem. Commun.* **2010**, *46*, 6950−6952. (h) Zhang, Y.; Tang, L.; Pullarkat, S. A.; Liu, F.; Li, Y.; Leung, P.-H. *J. Organomet. Chem.* **2009**, *694*, 3500−3505. (i) Yeo, W.-C.; Tee, S.-Y.; Tan, H.-B.; Tan, G.-K.; Koh, L. L.; Leung, P.-H. *Inorg. Chem.* **2004**, *43*, 8102−8109.

(6) (a) Kovacik, I.; Scriban, C.; Glueck, D. S. *Organometallics* **2006**, *25*, 536−539. (b) Scriban, C.; Glueck, D. S.; Zakharov, L. N.; Kassel, W. S.; DiPasquale, A. G.; Golen, J. A.; Rheingold, A. L. *Organometallics* **2006**, *25*, 5757−5767. (c) Scriban, C.; Kovacik, I.; Glueck, D. S. *Organometallics* **2005**, *24*, 4871−4874. (d) Costa, E.; Pringle, P. G.; Worboys, K. *Chem. Commun.* **1998**, 49−50. (e) Costa, E.; Pringle, P. G.; Smith, M. B.; Worboys, K. *J. Chem. Soc., Dalton Trans.* **1997**, 4277−4282. (f) Pringle, P. G.; Smith, M. B. *J. Chem. Soc., Chem. Commun.* **1990**, 1701−1702. (g) Wicht, D. K.; Kourkine, I. V.; Lew, B. M.; Nthenge, J. M.; Glueck, D. S. *J. Am. Chem. Soc.* **1997**, *119*, 5039−5040.

(7) (a) Geer, A. M.; Serrano, A. L.; de Bruin, B.; Ciriano, M. A.; Tejel, C. *Angew. Chem.* **2015**, *54*, 472−475. (b) Han, L.-B.; Tilley, T. D. *J. Am. Chem. Soc.* **2006**, *128*, 13698−13699. (c) Böhm, V. P. W.; Brookhart, M. *Angew. Chem., Int. Ed.* **2001**, *40*, 4694−4696.

(8) (a) Itazaki, M.; Nishihara, Y.; Osakada, K. *Organometallics* **2004**, *23*, 1610−1621. (b) Kovacik, I.; Wicht, D. K.; Grewal, N. S.; Glueck, D. S.; Incarvito, C. D.; Guzei, I. A.; Rheingold, A. L. *Organometallics* **2000**, *19*, 950−953. (c) Jaska, C. A.; Lough, A. J.; Manners, I. *Dalton Trans.* **2005**, 326−331.

(9) Ganushevich, Y. S.; Miluykov, V. A.; Polyancev, F. M.; Latypov, S. K.; Lönnecke, P.; Hey-Hawkins, E.; Yakhvarov, D. G.; Sinyashin, O. G. *Organometallics* **2013**, *32*, 3914−3919.

(10) (a) Nikonov, G. I.; Kuzmina, L. G.; Mountford, P.; Lemenovskii, D. A. *Organometallics* **1995**, *14*, 3588−3591. (b) Bonanno, J. B.; Wolczanski, P. T.; Lobkovsky, E. B. *J. Am. Chem. Soc.* **1994**, *116*, 11159−11160.

(11) Baker, R. T.; Calabrese, J. C.; Harlow, R. L.; Williams, I. D. *Organometallics* **1993**, *12*, 830−841.

(12) (a) Mastrorilli, P. *Eur. J. Inorg. Chem.* **2008**, *2008*, 4835−4850. (b) Alonso, E.; Casas, J. M.; Cotton, F. A.; Feng, X.; Forniés, J.; Fortuño, C.; Tomas, M. *Inorg. Chem.* **1999**, *38*, 5034−5040.

(13) (a) Forniés, J.; Fortuño, C.; Ibáñez, S.; Martín, A.; Mastrorilli, P.; Gallo, V.; Tsipis, A. *Inorg. Chem.* **2013**, *52*, 1942−1953. (b) Forniés, J.; Fortuño, C.; Ibáñez, S.; Martín, A.; Mastrorilli, P.; Gallo, V. *Inorg. Chem.* **2011**, *50*, 10798−10809. (c) Forniés, J.; Fortuño, C.; Ibáñez, S.; Martín, A. *Inorg. Chem.* **2008**, *47*, 5978−5987.

(14) (a) Arias, A.; Forniés, J.; Fortuño, C.; Martín, A.; Latronico, M.; Mastrorilli, P.; Todisco, S.; Gallo, V. *Inorg. Chem.* **2012**, *51*, 12682−12696. (b) Ara, I.; Forniés, J.; Fortuño, C.; Ibáñez, S.; Martín, A.; Mastrorilli, P.; Gallo, V. *Inorg. Chem.* **2008**, *47*, 9069−9080. (c) Forniés, J.; Fortuño, C.; Ibáñez, S.; Martín, A. *Inorg. Chem.* **2006**, *45*, 4850−4858. (d) Chaouche, N.; Forniés, J.; Fortuño, C.; Kribii, A.; Martín, A.; Karipidis, P.; Tsipis, A. C.; Tsipis, C. A. *Organometallics* **2004**, *23*, 1797−1810.

(15) Arias, A.; Forniés, J.; Fortuño, C.; Ibáñez, S.; Martín, A.; Mastrorilli, P.; Gallo, V.; Todisco, S. *Inorg. Chem.* **2013**, *52*, 11398−11408.

(16) Arias, A.; Forniés, J.; Fortuño, C.; Martín, A.; Mastrorilli, P.; Todisco, S.; Latronico, M.; Gallo, V. *Inorg. Chem.* **2013**, *52*, 5493−5506.

(17) (a) Mena, I.; Casado, M. A.; Polo, V.; García-Orduña, P.; Lahoz, F. J.; Oro, L. A. *Dalton Trans.* **2014**, *43*, 1609−1619. (b) Wang, K.; Emge, T. J.; Goldman, A. S. *Inorg. Chim. Acta* **1997**, *255*, 395−398. (c) Pinillos, M. T.; Elduque, A. I.; Berkovich, E.; Oro, L. A. *J. Organomet. Chem.* **1996**, *509*, 89−93. (d) Grushin, V. V.; Vymenits, A. B.; Yanovsky, A. I.; Struchkov, Y. T.; Vol'pin, M. E. *Organometallics* **1991**, *10*, 48−49. (e) Klingert, B.; Rheingold, A. L.; Werner, H. *Inorg. Chem.* **1988**, *27*, 1354−1358. (f) McGhee, W. D.; Foo, T.; Hollander, F. J.; Bergman, R. G. *J. Am. Chem. Soc.* **1988**, *110*, 8543−8545. (g) Werner, H.; Klingert, B. *Organometallics* **1988**, *7*, 911−917. (h) Targos, T. S.; Geoffroy, G. L.; Rheingold, A. L. *Organometallics* **1986**, *5*, 12−16. (i) Arif, A. M.; Jones, R. A.; Seeberger, M. H.; Whittlesey, B. R.; Wright, T. C. *Inorg. Chem.* **1986**, *25*, 3943−3949. (j) Schenck, T. G.; Milne, C. R. C.; Sawyer, J. F.; Bosnich, B. *Inorg. Chem.* **1985**, *24*, 2338−2344. (k) Fultz, W. C.; Rheingold, A. L.; Kreter, P. E.; Meek, D. W. *Inorg. Chem.* **1983**, *22*, 860−863.

(18) See, for example: (a) Downing, D. O.; Zavalij, P.; Eichhorn, B. W. *Inorg. Chim. Acta* **2011**, *375*, 329−332. (b) Bleeke, J. R.; Rohde, A. M.; Robinson, K. D. *Organometallics* **1995**, *14*, 1674−1680. (c) Bleeke, J. R.; Rohde, A. M.; Robinson, K. D. *Organometallics* **1994**, *13*, 401−403. (d) Arif, A. M.; Heaton, D. E.; Jones, R. A.; Kidd, K. B.; Wright, T. C.; Whittlesey, B. R.; Atwood, J. L.; Hunter, W. E.; Zhang, H. *Inorg. Chem.* **1987**, *26*, 4065−4073. (e) Gaudiello, J. G.; Wright, T. C.; Jones, R. A.; Bard, A. J. *J. Am. Chem. Soc.* **1985**, *107*, 888−897. (f) Burkhardt, E. W.; Mercer, W. C.; Geoffrey, G. L. *Inorg. Chem.* **1984**, *23*, 1779−1782. (g) Kreter, P. E.; Meek, D. W. *Inorg. Chem.* **1983**, *22*, 319−326. (h) Jones, R. A.; Wright, T. C. *Organometallics* **1983**, *2*, 1842−1845. (i) Jones, R. A.; Wright, T. C.; Atwood, J. L.; Hunter, W. E. *Organometallics* **1983**, *2*, 470−472. (j) Jones, R. A.; Norman, N. C.; Seeberger, M. H.; Atwood, J. L.; Hunter, W. E. *Organometallics* **1983**, *2*, 1629−1634.

(19) Tejel, C.; Sommovigo, M.; Ciriano, M. A.; López, J. A.; Lahoz, F. J.; Oro, L. A. *Angew. Chem., Int. Ed.* **2000**, *39*, 2336−2339.

(20) (a) Fryzuk, M. D.; Joshi, K.; Chadha, R. K.; Rettig, S. J. *J. Am. Chem. Soc.* **1991**, *113*, 8724−8736. (b) Fryzuk, M. D.; Joshi, K. *Organometallics* **1989**, *8*, 722−726. (c) Fryzuk, M. D.; Bhangu, K. *J. Am. Chem. Soc.* **1988**, *110*, 961−963.

(21) (a) Ebsworth, E. A. V.; Mayo, R. A. *J. Chem. Soc., Dalton Trans.* **1988**, 477−484. (b) Ebsworth, E. A. V.; Gould, R. O.; Mayo, R. A.; Walkinshaw, M. *J. Chem. Soc., Dalton Trans.* **1987**, 2831−2838. (c) Ebsworth, E. A. V.; Mayo, R. *Angew. Chem., Int. Ed. Engl.* **1985**, *24*, 68−70. (d) Schunn, R. A. *Inorg. Chem.* **1973**, *12*, 1573−1579.

(22) Deeming, A. J.; Doherty, S.; Marshall, J. E.; Powell, J. L.; Senior, A. M. *J. Chem. Soc., Dalton Trans.* **1993**, 1093−1100.

DOI: 10.1021/acs.inorgchem.5b02301
Inorg. Chem. 2016, 55, 828−839

(23) Gloaguen, Y.; Jacobs, W.; de Bruin, B.; Lutz, M.; van der Vlugt, J. I. *Inorg. Chem.* **2013**, *52*, 1682−1684.
(24) Martín, C.; Mallet-Ladeira, S.; Miqueu, K.; Bouhadir, G.; Bourissou, D. *Organometallics* **2014**, *33*, 571−577.
(25) (a) Camerano, J. A.; Casado, M. A.; Ciriano, M. A.; Tejel, C.; Oro, L. A. *Chem. - Eur. J.* **2008**, *14*, 1897−1905. (b) Casado, M. A.; Hack, V.; Camerano, J. A.; Ciriano, M. A.; Tejel, C.; Oro, L. A. *Inorg. Chem.* **2005**, *44*, 9122−9124.
(26) Representative examples: (a) Scriban, C.; Wicht, D. K.; Glueck, D. S.; Zakharov, L. N.; Golen, J. A.; Rheingold, A. L. *Organometallics* **2006**, *25*, 3370−3378. ([Pt(*R*,*R*-Me-Duphos)(Me)(PPh^{i}Bu)]: (2.243(3) and 2.372(4) Å). (b) Reference 6b. ([Pt(*R*,*R*-Me-Duphos)(Me)(PPh_2)]: (2.255(2) and 2.382(2) Å). (c) Reference 22. ([$IrCl_2(PMe_2Ph)_3(PH_2)$]: (2.378(3) and 2.440(3) Å). (d) Wicht, D. K.; Kovacik, I.; Glueck, D. S. *Organometallics* **1999**, *18*, 5141−5151. ([Pt(*S*,*S*-Chiraphos)(Me)(PPhIs)]: 2.2845(14) and 2.3622(15) Å). (e) Wicht, D. K.; Paisner, S. N.; Lew, B. M.; Glueck, D. S.; Yap, G. P. A.; Liable-Sands, L. M.; Rheingold, A. L.; Haar, C. M.; Nolan, S. P. *Organometallics* **1998**, *17*, 652−660 ([Pt(dppe)(Me)($PHMes_2$)]: (2.273(5) and 2.378(5) Å). [Pt(dppe)(Me)($PMes_2$)]: (2.287(2) and 2.351(2) Å)..
(27) Planas, J. G.; Hampel, F.; Gladysz, J. A. *Chem. - Eur. J.* **2005**, *11*, 1402−1416.
(28) (a) Zhuravel, M. A.; Glueck, D. S.; Zakharov, L. N.; Rheingold, A. L. *Organometallics* **2002**, *21*, 3208−3214. (b) Rogers, J. R.; Wagner, T. P. S.; Marynick, D. S. *Inorg. Chem.* **1994**, *33*, 3104−3110.
(29) Sizova, O. V.; Skripnikov, L. V.; Sokolov, A. Y.; Sizov, V. V. *Int. J. Quantum Chem.* **2009**, *109*, 2581−2590.
(30) Serrano, A. L.; Casado, M. A.; López, J. A.; Tejel, C. *Inorg. Chem.* **2013**, *52*, 7593−7607.
(31) Demerseman, B.; Renouard, C.; Le Lagadec, R.; Gonzalez, M.; Crochet, P.; Dixneuf, P. H. *J. Organomet. Chem.* **1994**, *471*, 229−239.
(32) [Fe]: (a) Weber, L.; Kleinebekel, S.; Lönnecke, P. *Z. Anorg. Allg. Chem.* **2002**, *628*, 803−809. (b) Ashby, M. T.; Enemark, J. H. *Organometallics* **1987**, *6*, 1323−1327. (c) McNamara, W. F.; Duesler, E. N.; Paine, R. T. *Organometallics* **1986**, *5*, 1747−1749. [Mo]: (d) Álvarez, M. A.; García, M. E.; Ruiz, M. A.; Suárez, J. *Angew. Chem., Int. Ed.* **2011**, *50*, 6383−6387. [W]: (e) Mercier, F.; Ricard, L.; Mathey, F. *Organometallics* **1993**, *12*, 98−103.
(33) Ashby, M. T.; Enemark, J. H. *Organometallics* **1987**, *6*, 1318−1323.
(34) Kubo, K.; Baba, T.; Mizuta, T.; Miyoshi, K. *Organometallics* **2006**, *25*, 3238−3244.
(35) Cuesta, L.; Gerbino, D. C.; Hevia, E.; Morales, D.; Navarro-Clemente, M. E.; Pérez, J.; Riera, L.; Riera, V.; Miguel, D.; del Río, I.; García-Granda, S. *Chem. - Eur. J.* **2004**, *10*, 1765−1777.
(36) Hevia, E.; Pérez, J.; Riera, V. *Organometallics* **2003**, *22*, 257−263.
(37) (a) Kondo, T.; Kaneko, Y.; Taguchi, Y.; Nakamura, A.; Okada, T.; Shiotsuki, M.; Ura, Y.; Wada, K.; Mitsudo, T.-A. *J. Am. Chem. Soc.* **2002**, *124*, 6824−6825. and references therein. (b) Filippou, A. C.; Rosenauer, T. *Angew. Chem., Int. Ed.* **2002**, *41*, 2393−2396.
(38) Burt, R.; Cooke, M.; Green, M. *J. Chem. Soc. A* **1970**, 2981−2986.
(39) Filippou, A. C.; Rosenauer, T.; Schnakenburg, G. *Perspectives in Organometallic Chemistry* **2003**, *287*, 120−135.
(40) (a) Padolik, L. L.; Gallucci, J. C.; Wojcicki, A. *J. Am. Chem. Soc.* **1993**, *115*, 9986−9996. (b) Padolik, L. L.; Gallucci, J.; Wojcicki, A. *J. Organomet. Chem.* **1990**, *383*, C1−C6.
(41) (a) Corrigan, P. A.; Dickson, R. S.; Fallon, G. D.; Michel, L. J.; Mok, C. *Aust. J. Chem.* **1978**, *31*, 1937−1951. (b) Corrigan, P. A.; Dickson, R. S. *Aust. J. Chem.* **1979**, *32*, 2147−2158.
(42) (a) Wong, W.; Singer, S. J.; Pitts, W. D.; Watkins, S. F.; Baddley, W. H. *J. Chem. Soc., Chem. Commun.* **1972**, 672−673. (b) Visser, J. P.; Ramakers-Blom, J. E. *J. Organomet. Chem.* **1972**, *44*, C63−C65.
(43) Foerstner, J.; Kakoschke, A.; Wartchow, R.; Butenschön, H. *Organometallics* **2000**, *19*, 2108−2113.
(44) See, for example: MacDougall, T. J.; Trepanier, S. J.; Dutton, J. L.; Ferguson, M. J.; McDonald, R.; Cowie, M. *Organometallics* **2011**, *30*, 5882−5893.
(45) Perrin, D. D.; Armarego, W. L. F. *Purification of Laboratory Chemicals*, 3rd ed.; Pergamon Press: Exeter, UK, 1988.
(46) Ahlrichs, R. *Turbomole Version 6.5*; Theoretical Chemistry Group, University of Karlsruhe.
(47) PQS version 2.4, 2001, Parallel Quantum Solutions, Fayettevile, AR; the Baker optimizer is available separately from PQS upon request: Baker, I. *J. Comput. Chem.* **1986**, *7*, 385−395.
(48) Budzelaar, P. H. M. *J. Comput. Chem.* **2007**, *28*, 2226−2236.
(49) (a) Lee, C.; Yang, W.; Parr, R. G. *Phys. Rev. B: Condens. Matter Mater. Phys.* **1988**, *37*, 785−789. (b) Becke, A. D. *J. Chem. Phys.* **1993**, *98*, 1372−1377. (c) Becke, A. D. *J. Chem. Phys.* **1993**, *98*, 5648−5652. (d) Calculations were performed using the Turbomole functional "b3-lyp", which is not completely identical to the Gaussian "B3LYP" functional.
(50) (a) Weigend, F.; Ahlrichs, R. *Phys. Chem. Chem. Phys.* **2005**, *7*, 3297−3305. (b) Weigend, F.; Häser, M.; Patzelt, H.; Ahlrichs, R. *Chem. Phys. Lett.* **1998**, *294*, 143−152.
(51) (a) Turbomole basisset library, Turbomole Version 6.5. (b) Andrae, D.; Haeussermann, U.; Dolg, M.; Stoll, H.; Preuss, H. *Theor. Chim. Acta* **1990**, *77*, 123−141.
(52) (a) Mayer, I. *Chem. Phys. Lett.* **1983**, *97*, 270−274. (b) Mayer, I. *Chem. Phys. Lett.* **1984**, *110*, 440−444. (c) Mayer, I. *Int. J. Quantum Chem.* **1986**, *29*, 73−84. (d) Mayer, I. *Int. J. Quantum Chem.* **1986**, *29*, 477−483. (e) Bridgeman, A. J.; Cavigliasso, G.; Ireland, L. R.; Rothery, J. *J. Chem. Soc., Dalton Trans.* **2001**, 2095−2108.
(53) (a) Gorelsky, S. I. *AOMix: Program for Molecular Orbital Analysis*; University of Ottawa, version 6.5, 2011; http://www.sg-chem.net/. (b) Gorelsky, S. I.; Lever, A. B. P. *J. Organomet. Chem.* **2001**, *635*, 187−196.
(54) Sheldrick, G. M. *SADABS*; Bruker AXS: Madison, WI, 1997.
(55) Sheldrick, G. M. *Acta Crystallogr., Sect. A: Found. Crystallogr.* **2008**, *64*, 112−122.
(56) Farrugia, L. F. *J. Appl. Crystallogr.* **1999**, *32*, 837−838.

DOI: 10.1021/acs.inorgchem.5b02301
Inorg. Chem. 2016, 55, 828−839